



Original Article

S100A8 accelerates wound healing by promoting adipose stem cell proliferation and suppressing inflammation

WeiGuo Su ^{a, †}, PingLi Wang ^{b, †}, QiQiang Dong ^c, ShengJun Li ^c, ShuiWang Hu ^{d, *}^a Wound Repair Department of Nankai University Affiliated Nankai Hospital, No.6, Changjiang Road, Tianjin 300110, PR China^b Department of Surgery, Department of Medicine, Henan Medical College, No.8, Shuanghu Avenue, Longhu Town, Zhengzhou 451191, PR China^c Zhengzhou Renji Hospital, No.25 Wenzhi Road, Zhengzhou 450000, PR China^d Guangdong Provincial Key Laboratory of Proteomics, Department of Pathophysiology, School of Basic Medical Sciences, Southern Medical University, 1023-1063 South Shatai Road, Guangzhou 510515, China

ARTICLE INFO

Article history:

Received 7 January 2022

Received in revised form

1 June 2022

Accepted 23 June 2022

Keywords:

Adipose-derived stem cells

S100A8

Skin wound healing

Proliferation

Migration

ABSTRACT

Adipose-derived stem cells (ADSCs) are stem cells with multidirectional differentiation potential isolated from adipose tissue. They have the same immunomodulatory effect as bone marrow mesenchymal stem cells in wound repair and immune regulation as bone marrow. The mechanism of action of ADSCs in skin wound repair has not been elucidated. S100A8 is a calcium and zinc binding protein, but its role in skin wound healing is rarely reported. We herein show that S100A8 overexpression significantly promoted ADSC proliferation and differentiation, whereas S100A8 knockdown yielded the opposite results. A skin injury model with bone exposure was created in rats by surgically removing the skin from the head and exposing the skull. The wounds were treated with S100A8-overexpressing or S100A8-knockdown ADSCs, and wound healing was monitored. The serum levels of the inflammation-related factors tumor necrosis factor- α and interleukin-6 were decreased significantly after S100A8 overexpression, while the angiogenic factor vascular endothelial growth factor and connective tissue generating factor showed the opposite trend. Histological staining revealed that granulation tissue neovascularization was more pronounced in wounds treated with S100A8-overexpressing ADSCs than that in the control group. We conclude that S100A8 promotes the proliferation of ADSCs and inhibits inflammation to improve skin wound healing.

© 2022, The Japanese Society for Regenerative Medicine. Production and hosting by Elsevier B.V. This is an open access article under the CC BY-NC-ND license (<http://creativecommons.org/licenses/by-nc-nd/4.0/>).

1. Introduction

Skin wound healing is a complex process involving blood coagulation, inflammation onset and progression, matrix synthesis, vascular regeneration, fibrous tissue proliferation, re-epithelialization, wound contraction, and tissue remodeling. All of these phenomena are intertwined and occur sequentially, encompassing a wide range of cellular and extracellular matrix changes [1,2]. The process of regeneration and repair is regulated by both genetic and environmental factors [3,4]. Cell proliferation, migration, differentiation, and apoptosis, extracellular matrix synthesis

and decomposition, and wound contraction and closure all involve the initiation, cascade, and termination of growth factor/cytokine signaling in the wounded area, coordinating with and antagonizing each other to participate in regulating wound repair [5,6].

Adipose-derived stem cells (ADSCs) are mesenchymal stem cells found in subcutaneous tissues [7] that can proliferate to and differentiate at repair damaged parts of the body while secreting cytokines to promote cell activation in response to external stimuli [8]. ADSCs have considerable migration capacity and can be rapidly recruited to wound sites to promote wound healing [9,10]. In addition, ADSCs and fibroblasts are major sources of extracellular matrix proteins that are involved in maintaining skin structure and function [11]. Given the availability of ADSCs in large quantities, their utilization in bone tissue repair and skin defect repair is increasing.

S100A8, also known as MRP8, is a Ca^{2+} binding protein belonging to the S100 family [12] that is involved in cytoskeletal

* Corresponding author.

E-mail address: cmxf0371@163.com (S. Hu).

Peer review under responsibility of the Japanese Society for Regenerative Medicine.

[†] These authors contributed equally to this work.

rearrangement and arachidonic acid metabolism [13,14]. During inflammation, S100A8 plays a key role in regulating the inflammatory response by stimulating the recruitment of leukocytes and inducing cytokine secretion [15,16]. S100A8 exhibits a dual role in regulating the course of inflammation. While research has primarily focused on the pro-inflammatory effects of S100A8, its anti-inflammatory effects should not be overlooked. S100A8 stimulates human monocytes to inhibit interleukin-6 (IL-6) and tumor necrosis factor- α (TNF- α) production by down-regulating the phosphorylation of p38 [17]. In addition, S100A8 binds to cytokines in a non-covalent manner as a way to capture cytokines. S100A8 has been shown to ameliorate lipopolysaccharide-induced liver injury by inhibiting the oxidative metabolism of neutrophils and scavenging reactive oxygen species (ROS) [18]. However, the effect of S100A8 in ADSCs remains unknown.

In this study, we investigated the role of S100A8 in regulating ADSCs. We show that S100A8 enhances wound healing by promoting the proliferation of ADSCs and suppressing inflammation.

2. Materials and methods

2.1. Cell culture and characterization

Rat ADSCs were purchased from Procell (CP-R198). The cells were cultured in a special medium for ADSCs (Procell, CM-R198) in a humidified atmosphere containing 5% CO₂ at 37 °C, and the medium was replaced every 2–3 days. When the cells reached 90% confluence, they were trypsinized using 0.05% trypsin and re-seeded in a new plate for various experiments. Cells were characterized using flow cytometry by double staining of CD45 (eBioscience, 12-0461-80) and CD105 (Invitrogen, MA1-19231).

2.2. Cell transfection

S100A8 (GI: 281485599) was used as the counterpart to construct S100A8 interference and overexpression vector, and the transfection efficiency was identified by Western blot after 24h transfection into ADSCs cells. To construct the S100A8 overexpression plasmids (op S100A8), rat-derived cDNA was cloned into the pcDNA3.1-EGFP vector, and empty pcDNA3.1-EGFP vectors by transient transfection and the empty pcDNA3.1-EGFP vector were used as a control (op CTL). The short hairpin-mediated S100A8 knockdown sequence (CCCTCAGTTTGTGCAGAATAAA) was engineered and cloned into the plvx-shRNA vector (sh S100A8), and a scrambled shRNA sequence (CGAGGGATGAGCCCGCTAGG) was used as a control (sh CTL).

2.3. Western blot

Cells were lysed and the proteins in the lysate were separated by sodium dodecyl sulfate-polyacrylamide gel electrophoresis and transferred to polyvinylidene fluoride membranes. The membranes were probed with antibodies against S100A8 (abcam, ab196680), glyceraldehyde 3-phosphate dehydrogenase (GAPDH, Bioswamp, PAB36269), connective tissue growth factor (CTGF, Bioswamp, PAB30609), vascular endothelial growth factor (VEGF, Bioswamp, PAB30096), nuclear factor- κ B (NF- κ B) (Bioswamp, PAB32144), pNF- κ B (Bioswamp, PAB43484-P), I κ B α (Bioswamp, PAB30687), pI κ B α (Abcam, ab133462) and then incubated with the corresponding secondary antibodies (goat anti-rabbit IgG, Bioswamp, SAB43714). A chemiluminescent agent was added to the membranes to visualize the protein signals, and images of the protein bands were captured using a luminescence system. The

proteins levels were quantified by ImageJ software (version 2, National Institutes of Health) and normalized by the internal control (GAPDH). The data represents the average of three independent replicates.

2.4. Wound healing

All animal handling protocols were approved by the Animal Ethics Committee of the Institutional Review Board at Wuhan Myhalic Biotechnological Co., Ltd (Approve number: HLK-20190417-01). Six-week-old male Sprague Dawley rats (n = 54), weighing approximately 200 g, were maintained in an automatic 12-h light/dark cycle and were fed standard food and water. All rats were observed daily for diet and mental status.

The rats were narcotized via isoflurane inhalation and complete anesthesia was ensured before starting the experiment. A round full-thickness wound (FSW) with a diameter of 0.8 cm was created on the scalp, exposing the skull. All wounds were fixed with 3M clear medical film (1.5 cm \times 1.5 cm) along the edge. The wounds were covered with polyurethane foam dressings and held in place with adhesives. The experiment was divided into five groups: FSW, FSW + ADSCs (sh S100A8), FSW + ADSCs (sh CTL), FSW + ADSCs (op S100A8), and FSW + ADSCs (op CTL). Rats in the FSW + ADSCs groups were injected with correspondingly treated ADSCs (1×10^5 cells per injection, 0.1 mL) with 20G needle at 2 mm from the wound a total of five times every three days until they were sacrificed on day 17. We used abdominal aortic blood collection to transfer blood into blood collection tubes containing procoagulants to prepare serum for subsequent studies.

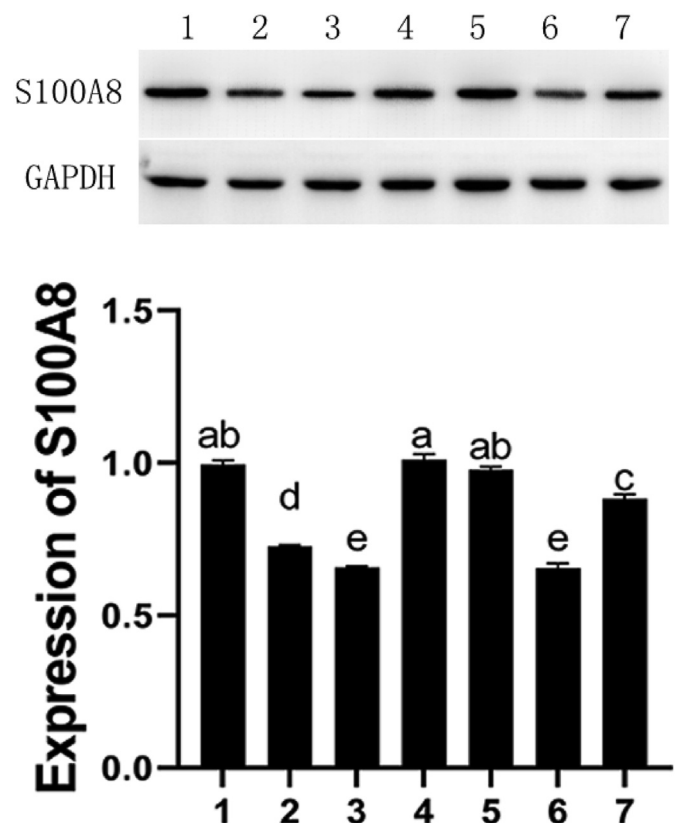


Fig. 1. Western blot assay of transfection efficiency of four plasmids. 1: control, 2: plasmid-1, 3: plasmid-2, 4: plasmid-3, 5: plasmid-4; 6: negative control, 7: positive control. Different letters indicate a difference between the two groups, $P < 0.05$.

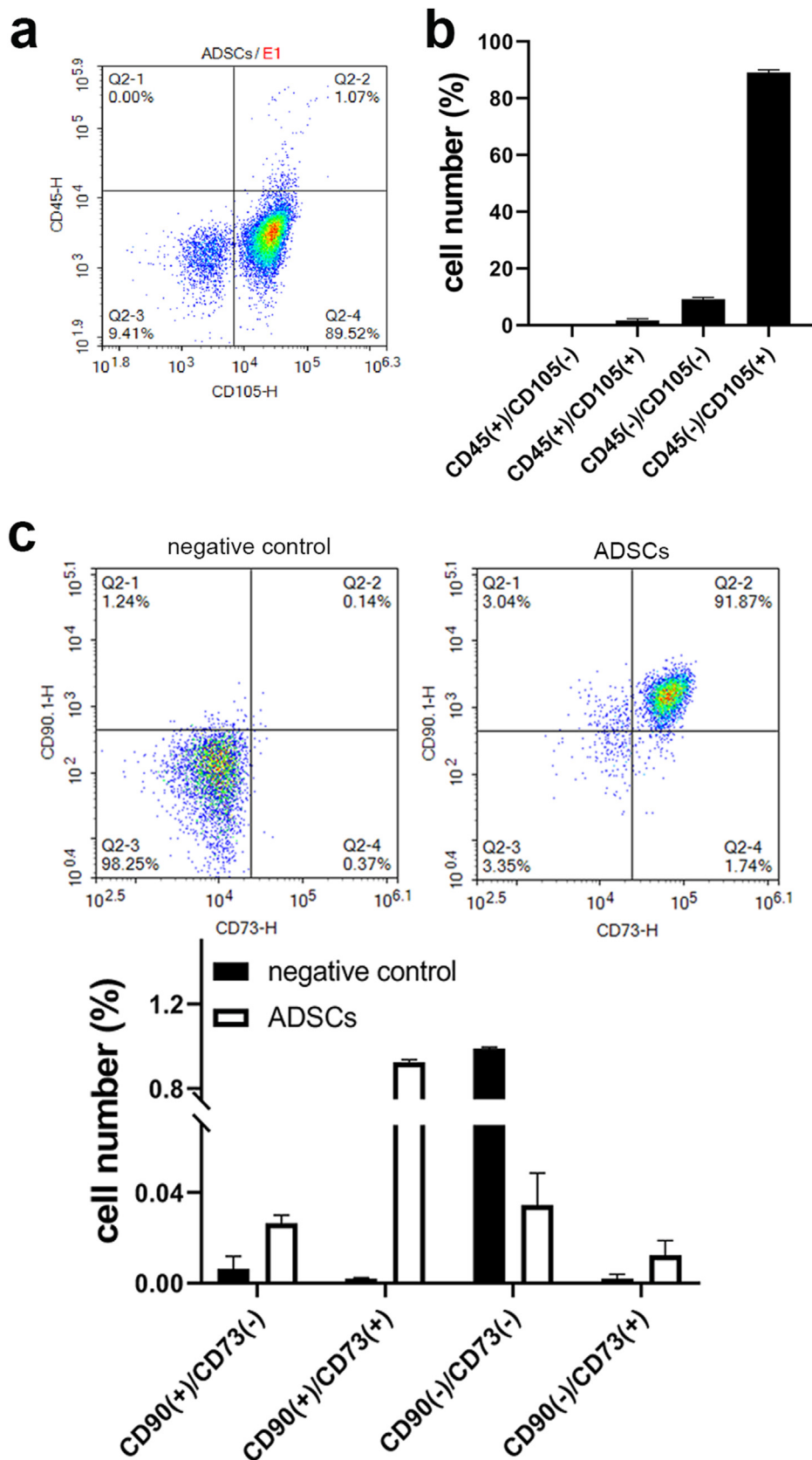


Fig. 2. Flow cytometric identification of ADSCs. (A) Diagram of flow cytometric sorting. (B) Proportion of cells with positive/negative expression of CD105 and/or CD45.

2.5. Enzyme-linked immunosorbent assay (ELISA)

Serum was collected from the rats after successful model construction to detect the protein levels of TNF- α , IL-6, VEGF, and CTGF according to the instructions of the ELISA kits (Bioswamp).

2.6. Proliferation assay

The Cell Counting Kit-8 assay (CCK-8) (CA1210; Solarbio Biotech) was performed to detect cell proliferation for the specified time period according to the manufacturer's protocol. Briefly, after S100A8 was overexpressed or knocked down, ADSCs were seeded into 96-well plates at a density of 3×10^3 cells per well. CCK-8 solution (10 μ l) was added to each well and the cells were incubated for an additional 4 h at 37 $^{\circ}$ C. The optical density of each well was measured at 450 nm.

2.7. Histological examination

After the rats were sacrificed, the injured tissues, including the surrounding 0.5 cm skin and the underlying skull, were carefully excised and fixed overnight in 4% formalin at 4 $^{\circ}$ C. The tissue was decalcified in the configured EDTA decalcification solution. After the decalcification was completed, paraffin-embedded tissues were sectioned. Tissue sections were stained with hematoxylin and eosin to detect wound status. Immunohistochemical staining

for CD34 (Bioswamp, PAB31801) and proliferating cell nuclear antigen (PCNA, Bioswamp, PAB30083) was performed according to the protocol of the immunohistochemistry kits (Maixin, KIT-5020).

2.8. Estimation of wound healing area

The sizes of the wounds were measured on day 0, 3, 12, and 17 after surgery. Images were photographed and analyzed quantitatively by ImageJ software.

2.9. Statistical analysis

The data are expressed as the mean \pm standard deviation. Comparisons between groups were performed by t-test or one-way analysis of variance. $p < 0.05$ was considered statistically significant. Statistical analysis was performed using SPSS version 23.0 (SPSS Inc.).

3. Results

3.1. Transfection efficiency assay

The expression of S100A8 protein was detected by Western Blot to verify the transfection efficiency. From Fig. 1, we know that

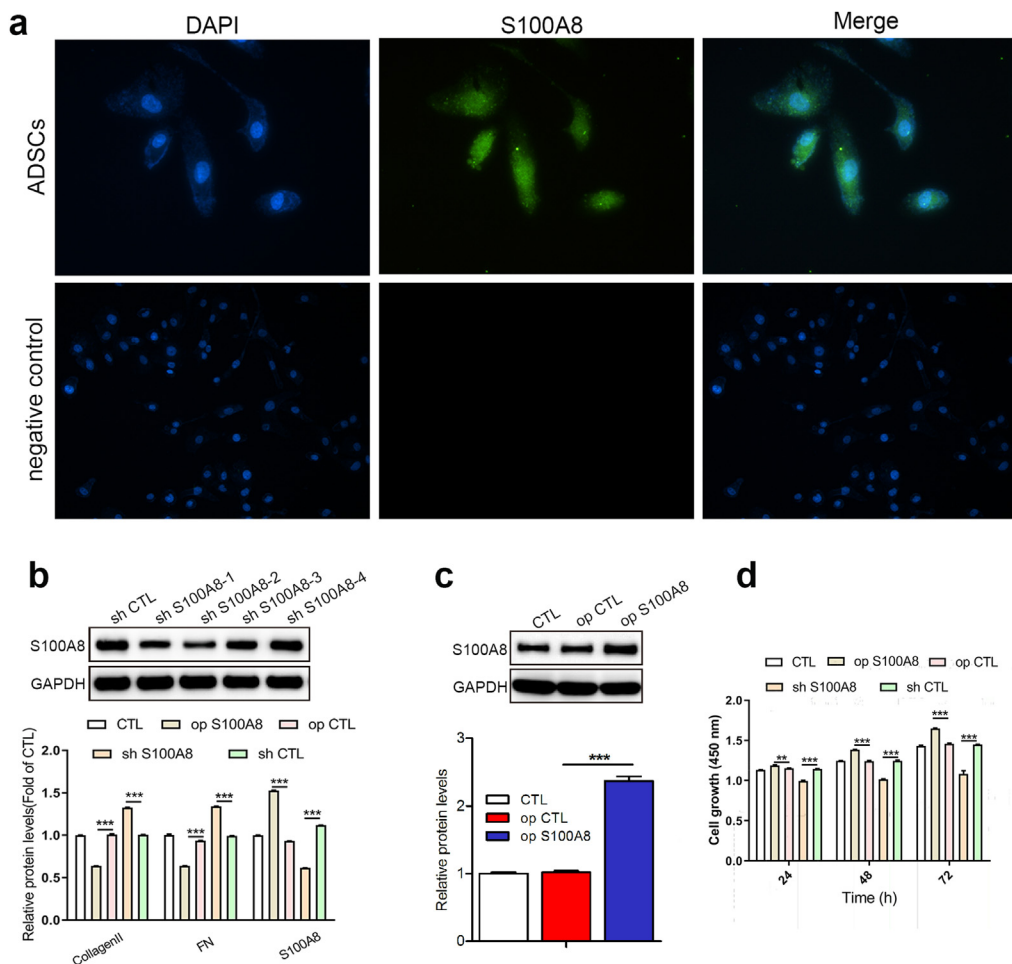


Fig. 3. S100A8 promotes ADSC proliferation. (A) Immunofluorescence detection of the expression and localization of S100A8 in ADSCs. Scale bar: 100 μ m. (B) S100A8 was knocked down in ADSCs, and the efficiency of knockdown was detected by Western blot. (C) S100A8 was overexpressed in ADSCs, and the efficiency of overexpression was detected by Western blot. (D) The proliferation of transfected ADSCs (overexpression or knockdown) was evaluated by CCK-8 assay. N = 3 animals/condition; * $P < 0.05$; ** $P < 0.01$; *** $P < 0.001$.

interference plasmid-2 has the best effect and its transfection efficiency is close to that of the negative control.

3.2. Identification of ADSCs

Biological characterization of ADSCs derived from rat abdominal fat was performed by flow cytometry. As shown in Fig. 2, ADSCs expressed high levels of the stem cell marker CD105 and CD73. And the expression of the hematopoietic cell marker CD90 was positive. In contrast, the expression of the hematopoietic cell marker CD45 was negative in ADSCs.

3.3. S100A8 overexpression promotes ADSC proliferation

As a calcium-binding protein, S100A8 plays a critical role in the development of inflammation. ADSCs are uniquely positioned to

fight inflammation and promote skin healing, but the role of S100A8 in ADSCs has been neglected. We detected the localization of S100A8 in ADSCs by immunofluorescence and observed that S100A8 was distributed in both the nucleus and cytoplasm (Fig. 3A). S100A8 was then overexpressed or knocked down in ADSCs (Fig. 3B–C). We found that S100A8 deficiency inhibited ADSC proliferation, while S100A8 overexpression showed the opposite result (Fig. 3D).

3.4. Overexpression of S100A8 in ADSCs accelerates wound healing

We have demonstrated that S100A8 accelerates the proliferation of ADSCs in vitro, but whether it promotes wound healing in vivo remains unknown. For this purpose, we constructed a full-layer skin lesion defect model in rats and the initial area of all wounds was approximately 0.5 cm² such as Fig. 4. The wound is

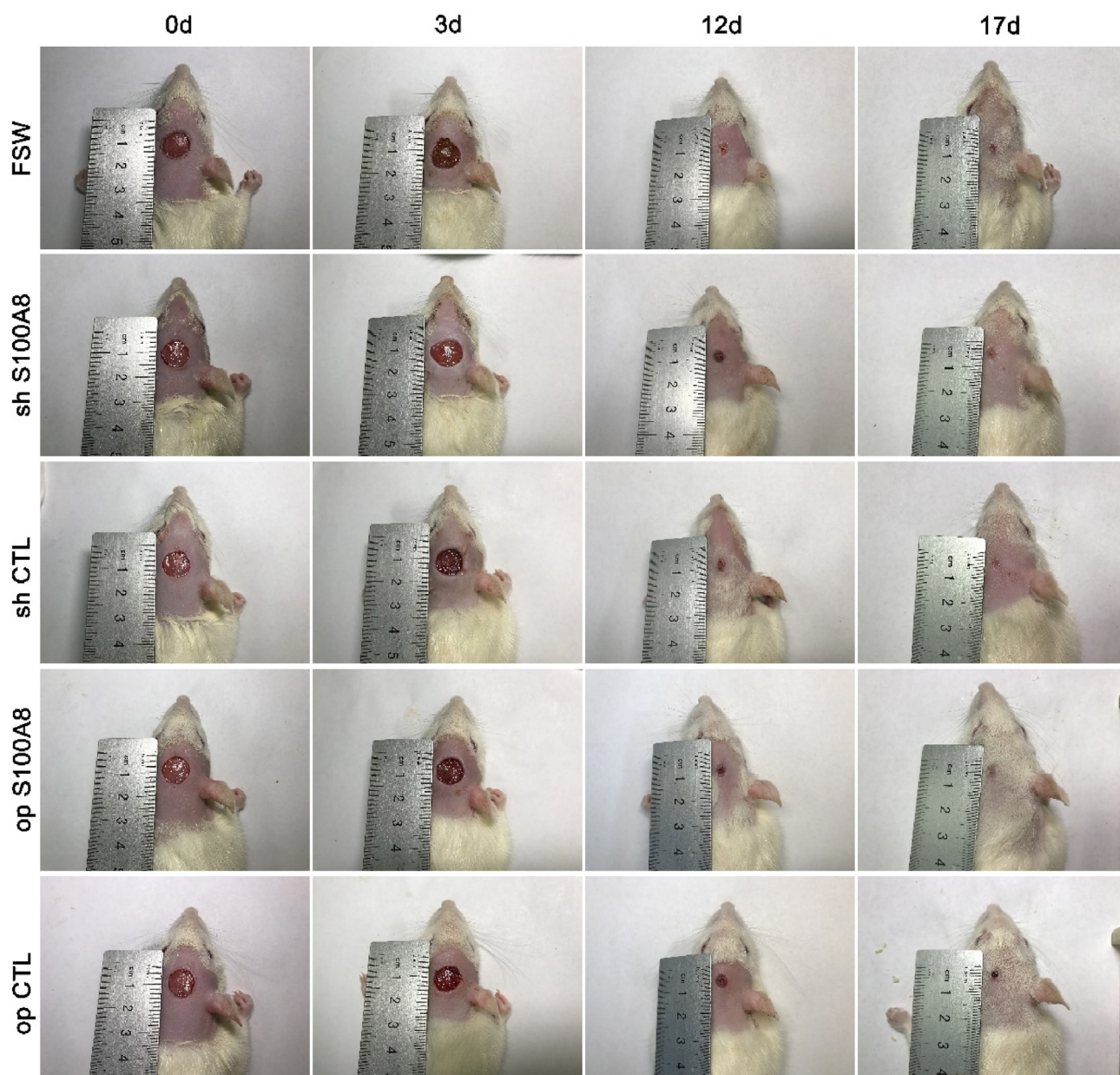


Fig. 4. Effect of ADSC transfection on the time course of wound closure. Representative appearance of skin healing in wounds treated with transfected ADSCs, on postoperative day 0, 3, 12, and 17. The rate of healing in wounds treated with transfected ADSCs (S100A8 knockdown or overexpression) on the first 3 days did not differ compared with that in the respective control groups. However, from day 3 to day 12, the rate of wound healing was higher in the S100A8 overexpression group. N = 3 animals/condition.

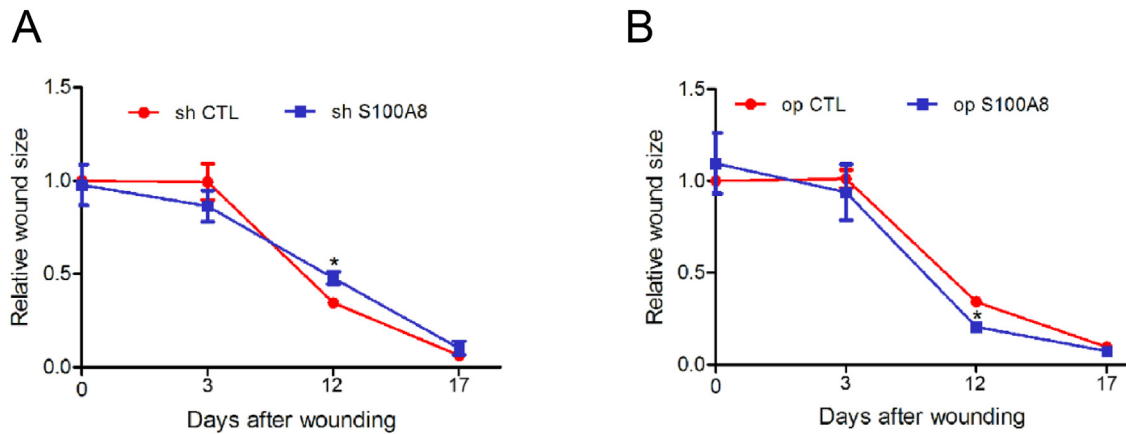


Fig. 5. Quantification of wound sizes for different treatments. Size of wounds treated with ADSCs subjected to S100A8 knockdown (A) and S100A8 overexpression (B). N = 3 animals/condition; **P* < 0.05.

quantified as shown in Fig. 5 shows wound healing on post-operative days 0, 3, 12, and 17 for each group. In op S100A8 group, fibroblast aggregation, angiogenesis, granulation tissue remodeling and epithelialization were more obvious than the other 4 groups, and the wound healing effect was the best. In addition, PCNA and CD34 protein expression was the highest. Compare with the op CTL group, the number of PCNA⁺ cells and blood vessel density in op S100A8 group were significantly higher (Fig. 6).

Filling wounds with S100A8-overexpressing ADSCs accelerated wound healing at 3 days postoperatively, but S100A8 knockdown in ADSCs impaired wound healing. Overall, the accelerating effect of S100A8 overexpression in ADSCs on wound healing was the most pronounced on postoperative days 3–12. By day 17, all wounds in rats receiving S100A8-overexpressing ADSCs were completely healed, whereas those in the control group were incompletely healed.

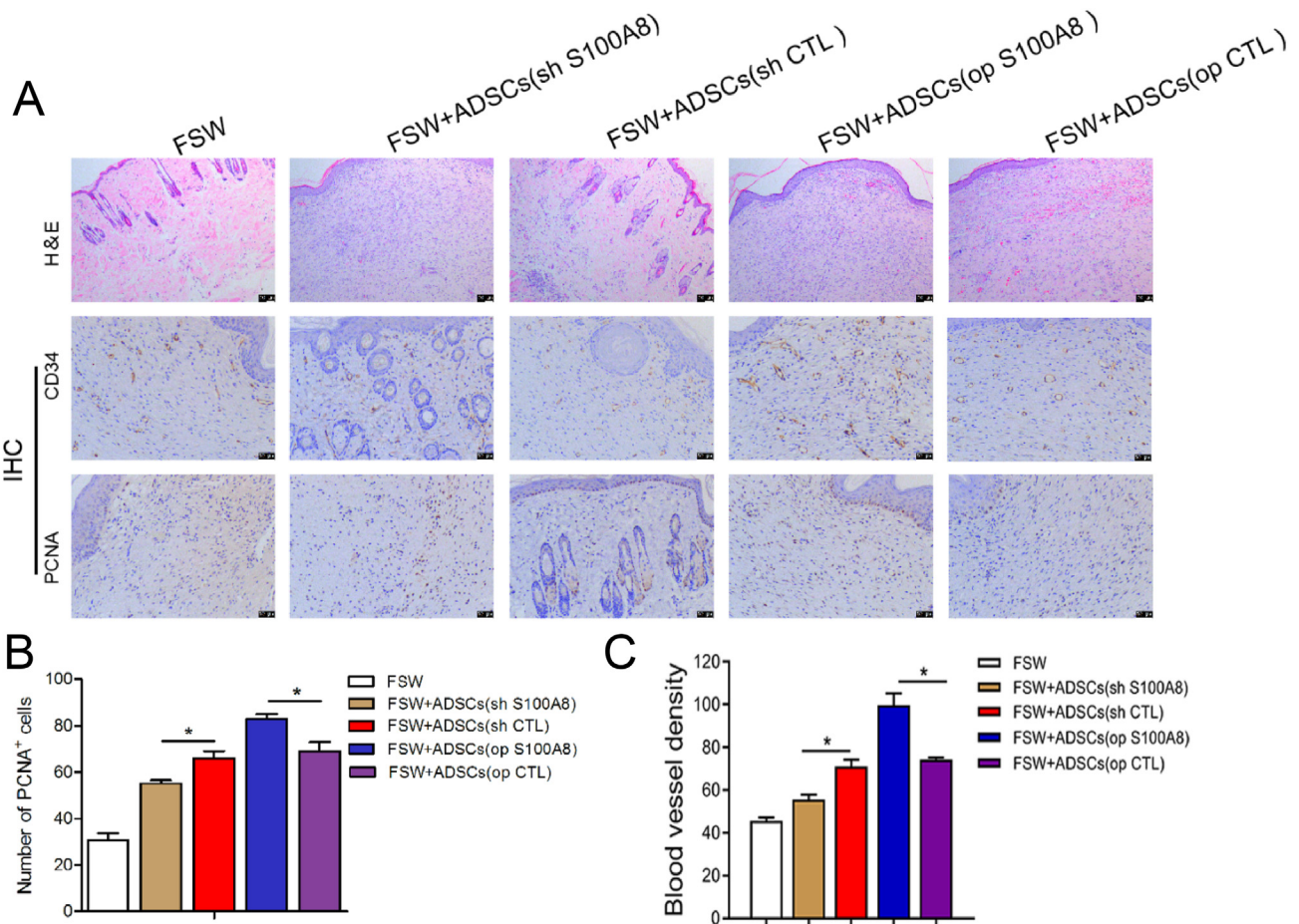


Fig. 6. Effects of ADSCs on granulation tissue formation. (A) Representative images of hematoxylin and eosin (H&E) staining in wound tissue sections. Immunohistochemical staining was performed for PCNA and CD34 in healing tissues after filling wounds with ADSCs. Scale bar: 100 μm. Number of cells with positive expression of CD34 (B) and PCNA (C) in healing tissues. N = 3 animals/condition; **P* < 0.05; ***P* < 0.01.

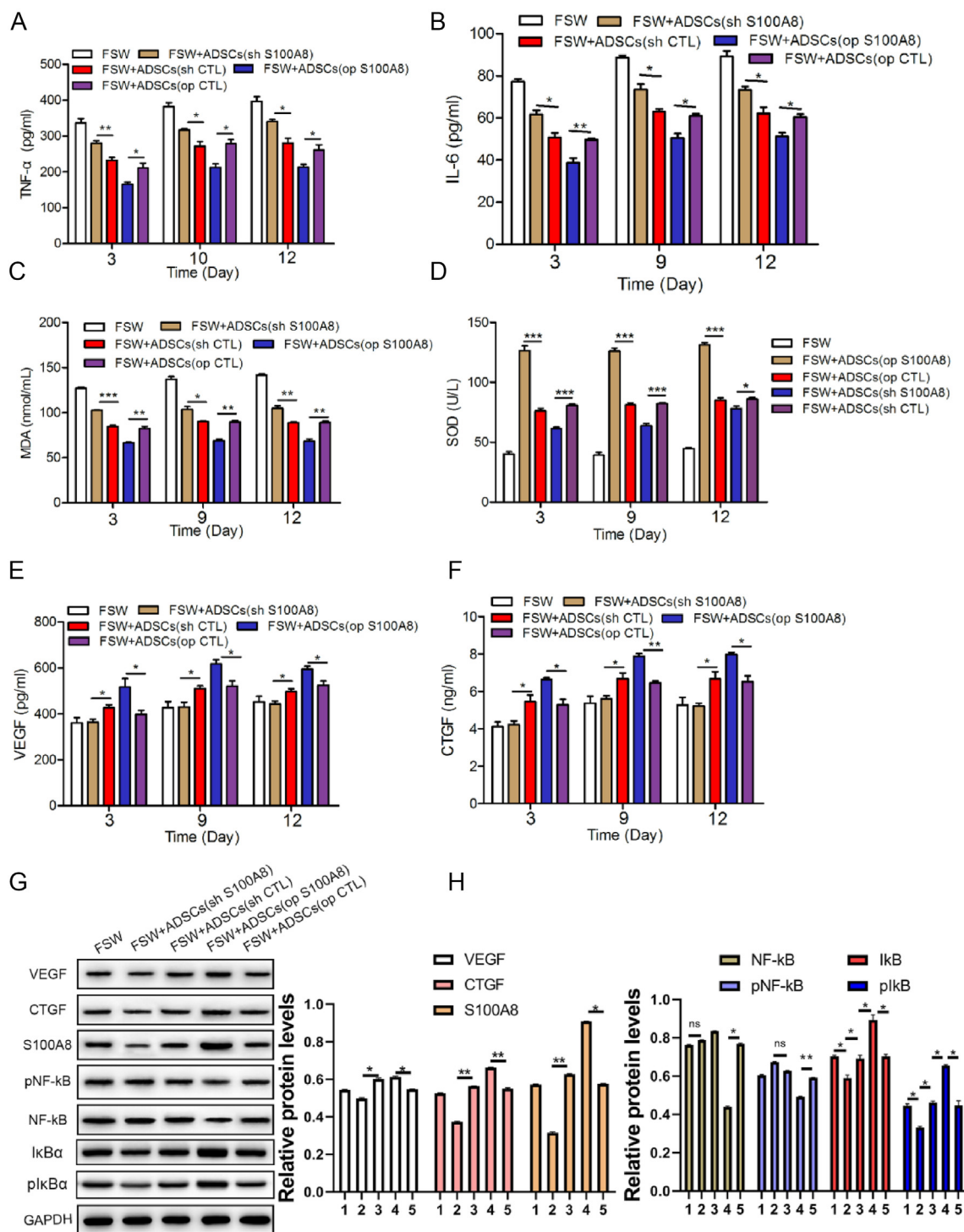


Fig. 7. S100A8 inhibits inflammation and oxidative stress. ELISA of the serum levels of TNF- α (A) and IL-6 (B). In rats treated with transfected ADSCs, the serum levels of oxidative stress-related factors MDA (C) and SOD (D) were detected by ELISA. As markers of wound healing, the expression of VEGF (E) and CTGF (F) was measured by ELISA. The expression of VEGF, CTGF, S100A8, NF- κ B, phosphorylated NF- κ B, I κ B α , phosphorylated I κ B α in healing tissue were detected by Western blot (G) and quantified (H), 1: FSW, 2: FSW + ADSCs (op S100A8), 3: FSW + ADSCs (op CTL), 4: FSW + ADSCs (sh S100A8), 5: FSW + ADSCs (sh CTL). N = 3 animals/condition; *P < 0.05; **P < 0.01.

3.5. S100A8 exhibits anti-inflammatory and anti-oxidant effects in wounds and promotes wound healing

After the wounds were filled with ADSCs, the serum levels of the inflammatory factors IL-6 and TNF- α were detected by ELISA at different time points (Fig. 7A and B). Compared with the control group, the serum levels of IL-6 and TNF- α in the S100A8 overexpression group were significantly reduced, while in the S100A8

deletion group, the levels of the two inflammatory factors were higher. Overexpression of S100A8 was able to increase serum superoxide dismutase (SOD) levels, while malondialdehyde (MDA) levels were significantly reduced compared to that in the controls (Fig. 7C and D).

The results of ELISA show that the levels of both wound healing factors were significantly increased in wounds treated with S100A8-overexpressing ADSCs (Fig. 7E and F). In addition, Western

blot confirmed that S100A8 enhanced the expression of VEGF and CTGF in the healing tissue, and the activation of the inflammation-related transcription factor NF- κ B was significantly inhibited whereas I κ B α and pI κ B α did not (Fig. 7G and H).

4. Discussion

Stem cell therapy is a valuable application in trauma management [20]. Stem cells come from a variety of sources including bone marrow, cord blood, amniotic fluid, and fat [21,22]. They have the capacity to differentiate into a variety of cell types such as chondrocytes, neuronal cells, osteoblasts, vascular endothelial cells, and fibroblasts [23,24]. ADSCs are easy to isolate because of their widespread origin, making them a potential resource for stem cell therapy [25,26] while their differentiation function has also been demonstrated [27]. Previous studies have shown that ADSCs responded to inflammatory stimuli, reduced or halted the expression of multiple inflammatory factors [28], migrated to sites of inflammation, and stimulated corresponding progenitor cells to promote proliferation and migration [29,30]. In addition, ADSCs have modulatory effects on immune responses and anti-inflammatory effects through the secretion of cytokines and growth factors that promote tissue repair [31,32]. These characteristics of ADSCs are the basis for their potential application in wound repair.

S100A8, a calcium-binding protein, plays a critical role in the occurrence and development of inflammation. Researchers have often focused on the pro-inflammatory properties S100A8 in understanding its activity. In inflammation induced by human infection, S100A8 is secreted in large quantities, and it exerts certain anti-bacterial properties when combined with Zn²⁺ [12,33]. Recently, the anti-inflammatory effect of S100A8 has been verified [34]. S100A8 has been shown to regulate the production of pro-inflammatory mediators, including cytokines, ROS, and nitric oxide [18,35]. It can reduce the secretion of IL-4, IL-6, and granulocyte-macrophage colony-stimulating factor by inhibiting the production of intracellular ROS in vitro. In the lungs of asthmatic mice, S100A8 inhibits eosinophil infiltration and chemokine production [34]. However, the role of S100A8 in wound healing is rarely reported. For wound healing, the benefits of stem cell therapy are obvious. In addition to the pluripotency of stem cells, the wide range of sources of stem cells, especially adipose tissues, is an advantage. Stem cell therapy can significantly enhance the healing ability of skin and greatly reduce healing time [36,37]. PCNA + can evaluate the formation of granulation tissue and thus determine wound healing [38]. Research on the adaptive response of ADSCs to S100A8 is unprecedented.

We explored the role of S100A8 in ADSCs in vitro and showed that S100A8 overexpression significantly promoted ADSC proliferation. Then, wounds were created in rats and filled with transfected ADSCs (knockdown or overexpression of S100A8). We observed that S100A8-overexpressing ADSCs significantly shortened the wound healing time, while S100A8 knockdown showed the opposite result. Wound healing undergoes four stages: hemostasis, inflammation, proliferation, and remodeling. Among them, the transition from the inflammatory to the proliferative phase is the most critical. Our previous results showed that S100A8 has the ability to promote granulation tissue formation. The function of S100A8 varies in different situations, but whether S100A8 in ADSCs plays an anti-inflammatory effect to promote wound healing remains unknown. In subsequent studies, we will work to investigate the mechanism of action of S100A8 in wound healing and anti-inflammation. We detected the expression of the pro-inflammatory factors IL-6 and TNF- α in the serum of rats treated with ADSCs by ELISA and the results are consistent with our

expectations. Compared with the control group, S100A8 overexpression significantly reduced the content of pro-inflammatory factors, whereas S100A8 knockdown increased the level of pro-inflammatory factors. In addition, VEGF and CTGF participate in wound healing by promoting angiogenesis and connective tissue formation, which are conducive to rapid wound healing. The levels of the angiogenesis marker VEGF and connective tissue generation marker CTGF were significantly increased after S100A8 was overexpressed. It has been reported that in the lungs of emphysema patients, low S100A8 expression is related to high oxidative stress [39]. In HIV patients, abnormal expression of S100A8 is a key factor affecting oxidative stress [40]. Previous studies have confirmed that moderate oxidative stress is essential for wound healing. Conversely, excessive oxidative stress delays wound healing by inhibiting angiogenesis and regulating extracellular matrix deposition [41]. However, whether S100A8 is involved in inhibiting oxidative stress during wound healing is unknown. We showed that S100A8 significantly reduced the serum concentration of MDA, but increased the activity of SOD.

However, this study has some limitations. We did not detect the activity of cells after transplantation into mice, and we were unable to determine how much of the spread of ADSC promoted by S100A8 was due to PCNA +. We will continue to delve into the issues in the follow-up study.

5. Conclusion

Collectively, our findings showed that S100A8 up-regulation promoted ADSC proliferation. In the inflammatory environment of wound healing, S100A8 in ADSCs suppressed the expression of the pro-inflammatory factors IL-6 and TNF- α to improve wound healing efficiency. In addition, S100A8 in ADSCs inhibited oxidative stress and protected the healing tissues from free radical attack, thereby promoting wound healing, providing a therapeutic strategy and direction for the clinical use of ADSCs in the treatment of wounds with exposed bone.

Ethics approval

All animal handling protocols were approved by the Animal Ethics Committee of the Institutional Review Board at Wuhan Myhalic Biotechnological Co., Ltd (Approve number: HLK-20190417-01).

Data availability statement

The datasets generated and/or analysed during the current study are not publicly available due article in preparation stage but are available from the corresponding author on reasonable request.

Author contributions

W.G.S. and S.W.H. conceived and designed the study. W.G.S., P.L.W., Q.Q.D., S.J.L. performed the experiments. W.G.S. wrote the paper. W.G.S., P.L.W., Q.Q.D., S.J.L. and S.W.H. reviewed and edited the manuscript. All authors read and approved the manuscript.

Funding

This work was supported by Guangdong Provincial Medical Science and Technology Research Project (A2017577).

Declaration of competing interest

The authors declare that the research was conducted in the absence of any commercial or financial relationships that could be construed as a potential conflict of interest.

References

- [1] Jun JI, Lau LF. Resolution of organ fibrosis. *J Clin Invest* 2018;128:97–107.
- [2] Yu J, Wang MY, Tai HC, Cheng NC. Cell sheet composed of adipose-derived stem cells demonstrates enhanced skin wound healing with reduced scar formation. *Acta Biomater* 2018;77:191–200.
- [3] Jhamb S, Vangaveti VN, Malabu UH. Genetic and molecular basis of diabetic foot ulcers: clinical review. *J Tissue Viability* 2016;25:229–36.
- [4] Lamster IB, Asadourian L, Del Carmen T, Friedman PK. The aging mouth: differentiating normal aging from disease. *Periodontol* 2000 2016;72:96–107.
- [5] Fui LW, Lok MPW, Govindasamy V, Yong TK, Lek TK, Das AK. Understanding the multifaceted mechanisms of diabetic wound healing and therapeutic application of stem cells conditioned medium in the healing process. *J Tissue Eng Regen Med* 2019;13:2218–33.
- [6] Wong W, Crane ED, Kuo Y, Kim A, Crane JD. The exercise cytokine interleukin-15 rescues slow wound healing in aged mice. *J Biol Chem* 2019;294:20024–38.
- [7] Wada Y, Ikemoto T, Morine Y, Imura S, Saito Y, Yamada S, et al. The differences in the characteristics of insulin-producing cells using human adipose-tissue derived mesenchymal stem cells from subcutaneous and visceral tissues. *Sci Rep* 2019;9:13204.
- [8] Zhou ZQ, Chen Y, Chai M, Tao R, Lei YH, Jia YQ, et al. Adipose extracellular matrix promotes skin wound healing by inducing the differentiation of adipose-derived stem cells into fibroblasts. *Int J Mol Med* 2019;43:890–900.
- [9] Zhang L, Zhang B, Liao B, Yuan S, Liu Y, Liao Z, et al. Platelet-rich plasma in combination with adipose-derived stem cells promotes skin wound healing through activating Rho GTPase-mediated signaling pathway. *Am J Transl Res* 2019;11:4100–12.
- [10] Mazini L, Rochette L, Admou B, Amal S, Malka G. Hopes and limits of adipose-derived stem cells (ADSCs) and mesenchymal stem cells (MSCs) in wound healing. *Int J Mol Sci* 2020:21.
- [11] Ebnerasuly F, Hajebrahimi Z, Tabaie SM, Darbouy M. Simulated microgravity condition alters the gene expression of some ECM and adhesion molecules in adipose derived stem cells. *Int J Mol Cell Med* 2018;7:146–57.
- [12] Wang S, Song R, Wang Z, Jing Z, Wang S, Ma J. S100A8/A9 in inflammation. *Front Immunol* 2018;9:1298.
- [13] van den Bos C, Roth J, Koch HG, Hartmann M, Sorg C. Phosphorylation of MRP14, an S100 protein expressed during monocytic differentiation, modulates Ca(2+)-dependent translocation from cytoplasm to membranes and cytoskeleton. *J Immunol* 1996;156:1247–54.
- [14] Kerkhoff C, Klempf M, Kaever V, Sorg C. The two calcium-binding proteins, S100A8 and S100A9, are involved in the metabolism of arachidonic acid in human neutrophils. *J Biol Chem* 1999;274:32672–9.
- [15] Kim MJ, Im MA, Lee JS, Mun JY, Kim DH, Gu A, et al. Effect of S100A8 and S100A9 on expressions of cytokine and skin barrier protein in human keratinocytes. *Mol Med Rep* 2019;20:2476–83.
- [16] Silveira AAA, Mahon OR, Cunningham CC, Corr EM, Mendonca R, Saad STO, et al. S100A8 acts as an autocrine priming signal for heme-induced human Mvarphi pro-inflammatory responses in hemolytic inflammation. *J Leukoc Biol* 2019;106:35–43.
- [17] Coveney AP, Wang W, Kelly J, Liu JH, Blankson S, Wu QD, et al. Myeloid-related protein 8 induces self-tolerance and cross-tolerance to bacterial infection via TLR4- and TLR2-mediated signal pathways. *Sci Rep* 2015;5:13694.
- [18] Sun Y, Lu Y, Engeland CG, Gordon SC, Sroussi HY. The anti-oxidative, anti-inflammatory, and protective effect of S100A8 in endotoxemic mice. *Mol Immunol* 2013;53:443–9.
- [20] Hsuan YC, Lin CH, Chang CP, Lin MT. Mesenchymal stem cell-based treatments for stroke, neural trauma, and heat stroke. *Brain Behav* 2016;6:e00526.
- [21] Ma Q, Liao J, Cai X. Different sources of stem cells and their application in cartilage tissue engineering. *Curr Stem Cell Res Ther* 2018;13:568–75.
- [22] Hosseini FS, Soleimanifar F, Ardeshiryajimi A, Vakilian S, Mossahebi-Mohammadi M, Enderami SE, et al. In vitro osteogenic differentiation of stem cells with different sources on composite scaffold containing natural bio-ceramic and polycaprolactone. *Artif Cell Nanomed Biotechnol* 2019;47:300–7.
- [23] Ding DC, Shyu WC, Lin SZ. Mesenchymal stem cells. *Cell Transplant* 2011;20:5–14.
- [24] Fu X, Liu G, Halim A, Ju Y, Luo Q, Song AG. Mesenchymal stem cell migration and tissue repair. *Cells* 2019;8.
- [25] Zhang W, Bai X, Zhao B, Li Y, Zhang Y, Li Z, et al. Cell-free therapy based on adipose tissue stem cell-derived exosomes promotes wound healing via the PI3K/Akt signaling pathway. *Exp Cell Res* 2018;370:333–42.
- [26] Zhou W, Lin J, Zhao K, Jin K, He Q, Hu Y, et al. Single-cell profiles and clinically useful properties of human mesenchymal stem cells of adipose and bone marrow origin. *Am J Sports Med* 2019;47:1722–33.
- [27] Su X, Liao L, Shuai Y, Jing H, Liu S, Zhou H, et al. MiR-26a functions oppositely in osteogenic differentiation of BMSCs and ADSCs depending on distinct activation and roles of Wnt and BMP signaling pathway. *Cell Death Dis* 2015;6:e1851.
- [28] Marfia G, Navone SE, Hadi LA, Paroni M, Berno V, Beretta M, et al. The adipose mesenchymal stem cell secretome inhibits inflammatory responses of microglia: evidence for an involvement of sphingosine-1-phosphate signaling. *Stem Cells Dev* 2016;25:1095–7.
- [29] Wang X, Wang H, Cao J, Ye C. Exosomes from adipose-derived stem cells promotes VEGF-C-dependent lymphangiogenesis by regulating miRNA-132/TGF-beta pathway. *Cell Physiol Biochem* 2018;49:160–71.
- [30] Qiu H, Liu S, Wu K, Zhao R, Cao L, Wang H. Prospective application of exosomes derived from adipose-derived stem cells in skin wound healing: a review. *J Cosmet Dermatol* 2020;19:574–81.
- [31] Zhao H, Shang Q, Pan Z, Bai Y, Li Z, Zhang H, et al. Exosomes from adipose-derived stem cells attenuate adipose inflammation and obesity through polarizing M2 macrophages and being in white adipose tissue. *Diabetes* 2018;67:235–47.
- [32] Yu S, Cheng Y, Zhang L, Yin Y, Xue J, Li B, et al. Treatment with adipose tissue-derived mesenchymal stem cells exerts anti-diabetic effects, improves long-term complications, and attenuates inflammation in type 2 diabetic rats. *Stem Cell Res Ther* 2019;10:333.
- [33] Damo SM, Kehl-Fie TE, Sugitani N, Holt ME, Rathi S, Murphy WJ, et al. Molecular basis for manganese sequestration by calprotectin and roles in the innate immune response to invading bacterial pathogens. *Proc Natl Acad Sci U S A* 2013;110:3841–6.
- [34] Zhao J, Endoh I, Hsu K, Tedla N, Endoh Y, Geczy CL. S100A8 modulates mast cell function and suppresses eosinophil migration in acute asthma. *Antioxidants Redox Signal* 2011;14:1589–600.
- [35] Ghavami S, Eshragi M, Ande SR, Chazin WJ, Klonisch T, Halayko AJ, et al. S100A8/A9 induces autophagy and apoptosis via ROS-mediated cross-talk between mitochondria and lysosomes that involves BNIP3. *Cell Res* 2010;20:314–31.
- [36] Aragona M, Dekoninck S, Rulands S, Lenglez S, Mascere G, Simons BD, et al. Defining stem cell dynamics and migration during wound healing in mouse skin epidermis. *Nat Commun* 2017;8:14684.
- [37] Dekoninck S, Blanpain C. Stem cell dynamics, migration and plasticity during wound healing. *Nat Cell Biol* 2019;21:18–24.
- [38] Weinreich J, Gren MS, Bilali E, Kleinman HK, Coerper S, K?Nigsrainer A, et al. Effects of isoniazid and niacin on experimental wound-healing. *Surgery* 2010;147:780–8.
- [39] Lin CR, Bahmed K, Criner GJ, Marchetti N, Tuder RM, Kelsen S, et al. S100A8 protects human primary alveolar type II cells against injury and emphysema. *Am J Respir Cell Mol Biol* 2019;60:299–307.
- [40] Schwartz R, Lu Y, Villines D, Sroussi HY. Effect of human immunodeficiency virus infection on S100A8/A9 inhibition of peripheral neutrophils oxidative metabolism. *Biomed Pharmacother* 2010;64:572–5.
- [41] Xian D, Song J, Yang L, Xiong X, Lai R, Zhong J. Emerging roles of redox-mediated angiogenesis and oxidative stress in dermatoses. *Oxid Med Cell Longev* 2019;2019:2304018.